



Cite this: *Org. Biomol. Chem.*, 2024, 22, 1613

Received 13th December 2023,
Accepted 29th January 2024
DOI: 10.1039/d3ob02035e

rsc.li/obc

Ir(triNHC) complexes catalyzed glycerol and alcohol dehydrogenative coupling, yielding diverse α -hydroxy acids. Unlike conventional conditions, Ir(triNHC) facilitated additional C–C bond formation after lactic acid production from glycerol, exhibiting high TOFs. This protocol successfully converted 1,2-propanediol and sorbitol into α -hydroxy acids, highlighting biomass-derived sources' potential as valuable platform chemicals.

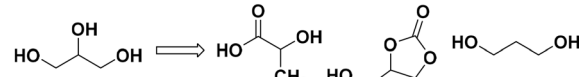
Global efforts to mitigate CO₂ concentration and combat climate change are currently underway. One effective strategy for reducing CO₂ emissions involves the development of fossil fuel-free chemical processes that utilize biomass-derived chemicals to produce industrially valuable compounds, thereby eliminating the need for additional fossil fuel consumption. By adopting this approach, we can significantly reduce greenhouse gas emissions while still meeting the demands of various industries.

Recent studies have highlighted the application of renewable biomass for diverse chemical transformations, focusing on glycerol.^{1–4} Glycerol, known for its non-toxic, biodegradable, and non-volatile properties, has emerged as a versatile resource for industrial chemical feedstocks and environmentally benign solvents. In the field of sustainable catalysis, there is a growing interest in utilizing glycerol for the synthesis of lactic acid, glycerol carbonate, and propanediol through transition-metal catalysis (Scheme 1).^{1–3} This interest stems from the fact that these products derived from glycerol are high-value-added products in the chemical industry.

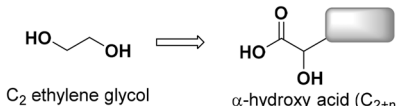
While most chemical conversions involving glycerol tend to preserve or reduce the number of carbons in the molecule (C₃ or less than C₃), it is important to explore innovative chemical methods capable of yielding a broader range of products from glycerol with increased carbon units. Recent advancements

have been made in the case of biomass-derived ethylene glycol, where protocols involving Ir-catalyzed dehydrogenation followed by aldol reactions have been employed to extend the carbon chain of ethylene glycol,^{5–11} leading to the synthesis of industrially valuable α -hydroxy acids (AHAs), as depicted in Scheme 1.^{12,13} Aliphatic AHAs are present in biologically interesting molecules, including lipoxazolidinone B (Scheme 1).^{14–16} Given the structural similarity between ethylene glycol and glycerol, it is expected that a comparable approach can elongate the carbon chain of glycerol.^{17–22} However, there is no report

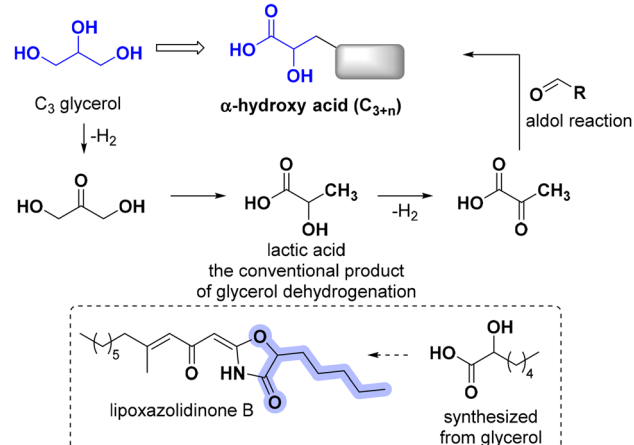
previously reported chemical conversions of glycerol



previous our work using ethylene glycol



this work: utilization of glycerol as sustainable C3 platform chemical



Department of Energy Systems Research, Ajou University, Suwon 16499, Korea.

E-mail: hyjang@ajou.ac.kr; Tel: +82(031)-219-2555

† Electronic supplementary information (ESI) available. See DOI: <https://doi.org/10.1039/d3ob02035e>



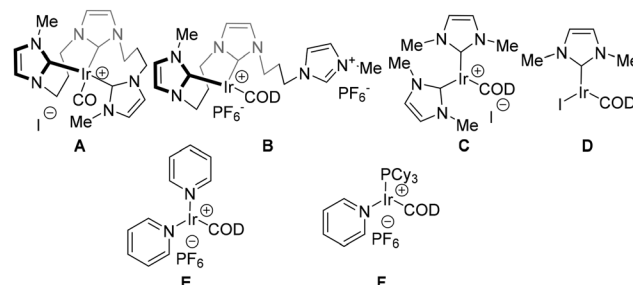
on a catalytic protocol for synthesizing higher C_n AHAs from glycerol to date. Unlike ethylene glycol, dehydrogenated glycerol readily undergoes the Cannizzaro reaction, forming lactic acid rather than facilitating C–C bond formation. In this study, we delve into the subsequent transformation of lactic acid, generated from glycerol, to produce AHAs *via* a dual process involving lactic acid dehydrogenation and aldol reactions (Scheme 1).^{23–25} Through this approach, we overcome the limitations posed by the Cannizzaro reaction of dehydrogenated glycerol and open the potential for AHA synthesis from biomass-derived glycerol.

Our research efforts have been dedicated to exploring the potential of Ir(NHC) (NHC = N-heterocyclic carbene)-catalyzed dehydrogenation and dehydrogenative coupling reactions of biomass-derived alcohols.^{5,26–28} Through our investigations, we have observed that incorporating NHC ligands into Ir catalysts yields a remarkable enhancement in their catalytic activity, particularly dehydrogenation reactions involving biomass-derived alcohols.²² This observation has led us to anticipate that Ir catalysts coordinated with NHC ligands could effectively facilitate the dehydrogenation of glycerol and lactic acid, both of which possess the alcohol functional group. Accordingly, the reaction of glycerol and benzyl alcohol was examined under Ir-catalyzed dehydrogenation conditions (Table 1). Ir(NHC) catalyst A (0.00625 mol%)²⁸ was used for the dehydrogenative cross-coupling of glycerol and benzyl alcohol at 180 °C in the presence of bases. Inorganic bases including LiOH, NaOH, KOH, CsOH·H₂O, Ba(OH)₂, and K₂CO₃ were examined (entries 1–6), with the highest turnover frequency (TOF) and a yield of **1b** observed in the presence of NaOH (entry 2). The evolution of H₂ was monitored with reactions using LiOH, NaOH, KOH, and CsOH·H₂O, exhibiting that NaOH-mediated reaction produced H₂ with the highest rate (Fig. 1a). The higher H₂ evolution rate showed a higher yield of **1b** (NaOH > KOH > CsOH > LiOH) (Fig. 1a and b). The TOF values of H₂ were higher than those of **1b**, suggesting that some dehydrogenated glycerol and benzyl alcohol did not participate in the further reaction to form **1b**. Upon NMR analysis of the reaction mixture of entry 2 of Table 1, it was noted that stoichiometric quantities of benzyl alcohol were consumed. This observation implies that the excess hydrogen generated is not a result of the over-dehydrogenation of benzyl alcohol. Intermediate lactic acid was not observed in the reaction mixture using NaOH, but a substantial amount of lactic acid was observed in other base-mediated reactions (Fig. 1b and Table S1†). The dehydrogenative coupling of **1b** with another molecule of benzyl alcohol yielded **1c** as a minor product. Increasing catalyst loadings slightly improved the yield but decreased the TOF (entry 7). Reducing the reaction temperature to 150 °C resulted in a significant reduction in both TOF and yield (entry 8). Increasing the amount of bases did not have a notable impact on the yield of **1b** (entry 9). Decreasing the amount of bases led to diminished yields and TOFs for **1b** and H₂, leaving a significant amount of lactate unconverted (entry 10 of Table 1 and Table S1†). To evaluate the effect of chelating tridentate NHC ligand, we employed catalysts **B**, **C**,

Table 1 Ir(NHC)-catalyzed dehydrogenative coupling of glycerol and benzyl alcohol

Entry	Catalyst	Base (equiv.)	Temp. (°C)	1b TOF (h ⁻¹), yield (%)	1c TOF (h ⁻¹)	H ₂ TOF (h ⁻¹)
1	A	LiOH (1.5)	180	—	—	2500
2	A	NaOH (1.5)	180	5100, 64	150	11 100
3	A	KOH (1.5)	180	3000, 38	190	10 600
4	A	CsOH·H ₂ O (1.5)	180	1400, 18	310	10 500
5	A	Ba(OH) ₂ (1.5)	180	—	—	1600
6	A	K ₂ CO ₃ (1.5)	180	—	—	1600
7	A ^a	NaOH (1.5)	180	2700, 68	170	7000
8	A	NaOH (1.5)	150	680, 8.5	—	4900
9	A	NaOH (3.0)	180	5200, 65	240	30 000
10	A	NaOH (1.0)	180	2200, 28	—	8200
11	B	NaOH (1.5)	180	5300, 66	—	10 800
12	C	NaOH (1.5)	180	—	—	1800
13	D	NaOH (1.5)	180	—	—	1500
14	E	NaOH (1.5)	180	—	—	1000
15	F	NaOH (1.5)	180	—	—	1100
16	—	NaOH (1.5)	180	—	—	2100

Reaction conditions: the mixture of catalysts (0.00625 mol%), glycerol (10 mmol), benzyl alcohol (7 equiv.), and base was heated. The yields and TOFs were determined by ¹H NMR using isonicotinic acid as an internal standard. ^a 0.0125 mol% of catalyst **A**.



and **D**.^{26,29,30} Catalyst **B** exhibited a comparable yield and a rate to catalyst **A** (entry 11), attributed to the *in situ* formation of a triNHC complex (Fig. 1c and Fig. S1†). Catalysts **C** and **D**, which featured non-chelating NHC ligands, did not form products (entries 12 and 13). The rates of H₂ production were much slower than those of catalysts **A** and **B** (Fig. 1c). Iridium catalysts **E** and **F** without NHC ligands failed to produce **1b** or **1c** (entries 14 and 15). While catalysts **C**–**F** did not promote desired cross-coupling reactions, lactic acid was formed in low yields (Fig. 1d and Table S1†). Finally, no product was observed in the absence of iridium catalysts (entry 16).³¹ We conducted a large-scale reaction using 100 mmol (9.2 g) of glycerol, which demonstrated a yield and TOF (53% and 4200 h⁻¹) comparable to those obtained in the 10 mmol glycerol reaction (entry 2, Table 1).

A plausible reaction mechanism involving double-dehydrogenations of glycerol to pyruvate and aldol reaction of pyruvate and benzaldehyde is depicted in Scheme 2. Glycerol, benzyl

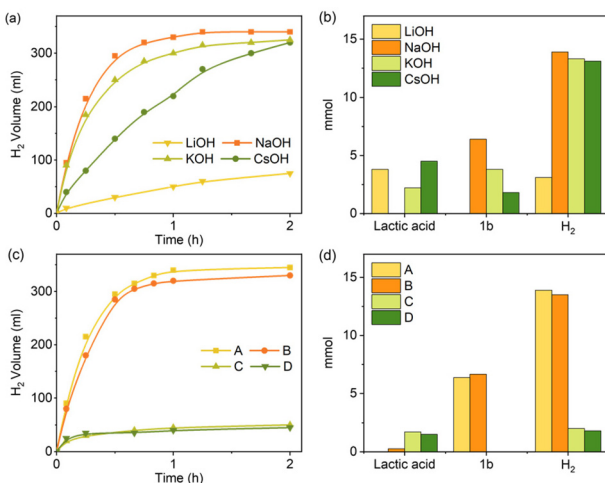
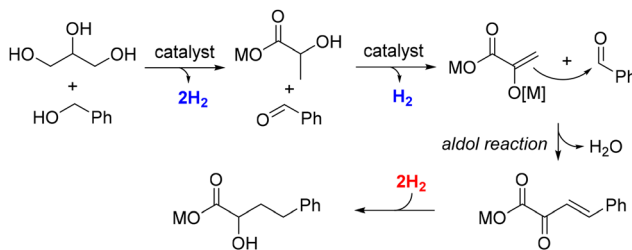


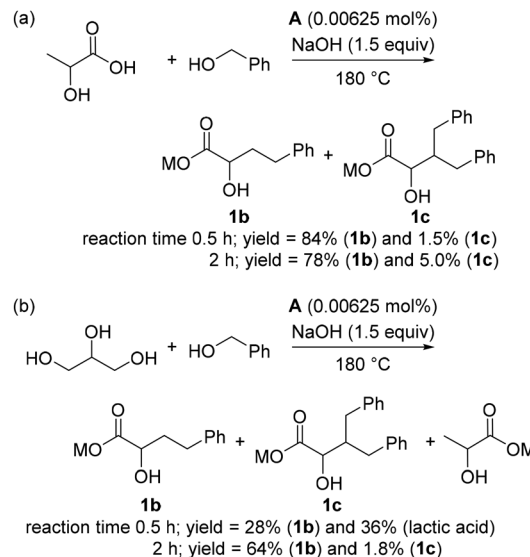
Fig. 1 (a) Time course plots of H₂ evolution from the coupling reactions of glycerol and benzyl alcohol using different bases, (b) the amount (mmol) of lactic acid, **1b**, and H₂ of the reactions using different bases, (c) time course plots of H₂ evolution from the coupling reactions of glycerol and benzyl alcohol using different catalysts (A–D), and (d) the amount (mmol) of lactic acid, **1b**, and H₂ of the reactions using different catalysts (A–D).



Scheme 2 Proposed reaction mechanism accompanying H₂ generation.

alcohol, and lactate undergo dehydrogenation to yield 3 molecules of H₂, while the hydrogenation of aldol products consumes 2 molecules of H₂. As a result, 1 molecule of H₂ is liberated within a catalytic cycle, provided there is no additional dehydrogenation without concurrent C–C bond formation. The observed amount of H₂ in entry 2 of Table 1 is approximately 1.4 equivalents to glycerol, implying that dehydrogenation of glycerol and benzyl alcohol without forming C–C bond-forming products occurs.

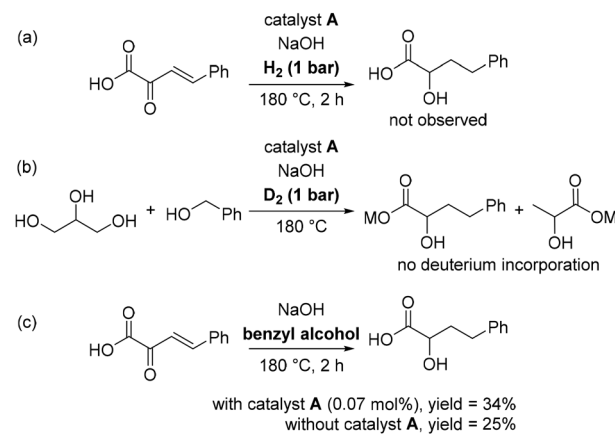
The control experiments were conducted to validate the proposed mechanism (Scheme 3). The reactions involving lactic acid and benzyl alcohol were conducted for different durations; 0.5 h and 2 h. It was observed that the cross-coupling reaction of lactic acid and benzyl alcohol reached completion within 0.5 h. Interestingly, the yield of **1b** in the 0.5 h-reaction exceeded that in the 2 h-reaction, attributed to the delayed benzylation of **1b** to form **1c** during the shorter reaction time. When glycerol and benzyl alcohol were reacted for 0.5 h, **1b** was obtained with a 28% yield, along with lactate at a 36% yield. Analysis of the ¹H NMR spectrum of the reaction mixture involving catalyst A (1 mol%) revealed the co-existence



Scheme 3 (a) Reaction of lactic acid with benzyl alcohol for different durations, (b) reaction of glycerol with benzyl alcohol for different durations.

of glycerol, lactic acid, and **1b** in a 1 : 4.2 : 2.8 ratio after just 7 min of reaction time (see ESI, Fig. S2†). Notably, lactate formed from glycerol readily engaged in cross-coupling with benzaldehyde, while concurrent dehydrogenation of glycerol and benzyl alcohols occurs.

Although the consumption of H₂ gas to reduce the aldol product is depicted (Scheme 2), it should be investigated whether the released H₂ molecules or Ir-monohydride formed from β -hydride elimination reduces the double bond and the carbonyl group of intermediates. The separated synthesized 2-oxo-4-phenylbut-3-enoic acid, when subjected to hydrogenation conditions, did not yield any desired product (Scheme 4a). Similarly, when glycerol and benzyl alcohol were reacted in the presence of D₂, no deuterium-incorporated products were observed (Scheme 4b). This outcome suggests that



Scheme 4 Reactions using additional hydrogen gas and benzyl alcohol as a hydride source.



the released hydrogen does not contribute to the reduction of aldol products. When 2-oxo-4-phenylbut-3-enoic acid was exposed to the reaction conditions involving benzyl alcohol as a hydride source, the desired product was observed (Scheme 4c). Notably, the desired reduction occurred both in the presence and absence of catalyst **A**, albeit with slightly higher product yield when catalyst **A** was employed.

Based on the findings from Scheme 4, it is evident that the released H_2 does not, notably, integrate into the subsequent catalytic cycle responsible for reducing the intermediates formed during the cross-coupling of lactic acid and benzaldehyde. The aldol product reduction primarily occurs through base-mediated transfer hydrogenation.^{32,33} The plausible catalytic cycles are elucidated in Fig. 2. The dehydrogenation of glycerol, benzyl alcohol, and lactate is initiated by intermediate **I**, leading to the formation of Ir(triNHC)-H species

(intermediates **III** and **V**), as illustrated in Fig. 2a and b. The reduction of the aldol condensation product is facilitated by NaOH-mediated transfer hydrogenation, using benzyl alcohol as a hydride source, as supported by the experimental results in Scheme 4c (Fig. 2c). Additionally, the presence of Ir(triNHC)-H species may expedite the reduction process, resulting in the formation of the desired product **1b**. Based on empirical results of entries 1–6 (Table 1) and mechanistic studies, the significance of bases emerges as pivotal in facilitating the dehydrogenative coupling reaction, participating in various key steps. Kinetic experiments were conducted, exhibiting a reaction order of 1.9 with respect to $[NaOH]$ (see ESI, Fig. S3†).

To observe the iridium intermediates through electrospray ionization-mass spectrometry (ESI-MS) analysis, a higher concentration of catalyst **A** was employed in the reactions involving glycerol and benzyl alcohol as well as lactic acid and benzyl alcohol. The observed species from the ESI-MS spectra of the reaction involving glycerol and benzyl alcohol were found to be similar to those from the reaction of lactic acid and benzyl alcohol (see ESI, Fig. S4 and S5†). The dehydrogenated catalyst **A** without CO (m/z 503.15); catalyst **A** – $[2H]^{34}$ and catalyst **A**

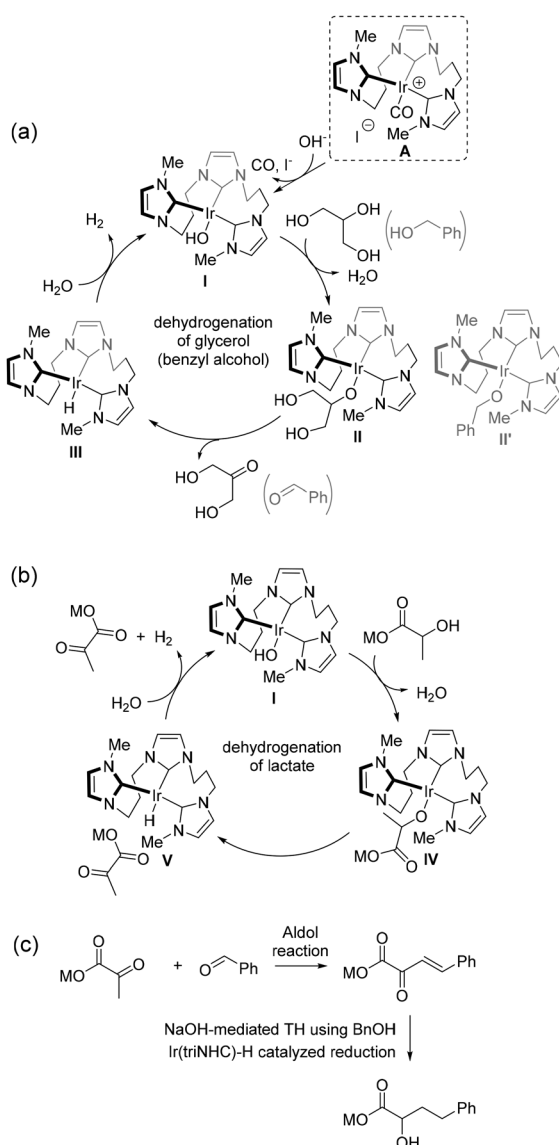


Fig. 2 Proposed mechanisms (a) dehydrogenation of alcohol, (b) dehydrogenation of lactate, and (c) cross-coupling and reduction.

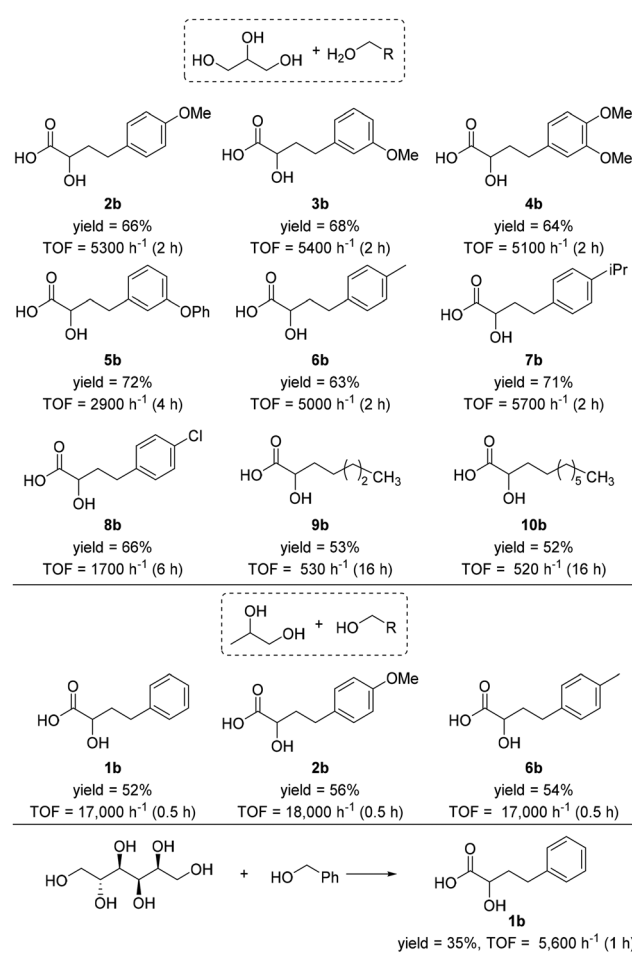


Fig. 3 The coupling reactions of glycerol (1,2-propanediol and sorbitol) with alcohols.



(*m/z* 533.16) were observed as major species, while Ir(triNHC)-H or Ir(triNHC)-2H coordinated with aldehyde and acid intermediates were observed as minor species in ESI-MS (see ESI, Fig. S4 and S5†).

The substrate scope exploration is depicted in Fig. 3, with a focus on various types of alcohols. Electron-rich benzyl alcohols involving methoxy groups on the phenyl ring were examined, rendering desired products **2b**, **3b**, and **4b** with yields (TOFs) of 66% (5300 h^{-1}), 68% (5400 h^{-1}), and 64% (5100 h^{-1}), respectively. Phenoxy, methyl, and isopropyl group-substituted products **5b**, **6b**, and **7b** were formed with comparable yields and TOFs. The electron-deficient Cl-substituted product **8b** exhibited a 66% yield but a lower TOF (1700 h^{-1}). Introducing aliphatic alcohols (butanol and heptanol) into the reaction produced products **9b** and **10b** with TOFs of 530 h^{-1} and 520 h^{-1} , respectively. Notably, aliphatic alcohols required extended reaction times for the complete consumption of lactic acid intermediates compared to their benzyl-substituted alcohols. Investigating beyond glycerol, we explored other biomass-derived polyols that could potentially generate lactate intermediates during the Ir(triNHC)-catalyzed dehydrogenation. In particular, 1,2-propanediol was subjected to this reaction, anticipating its transformation to lactic acid under basic dehydrogenation conditions.²⁹ This led to the enhanced formation of desired products **1b**, **2b**, and **6b**, demonstrating significantly higher TOFs. Sorbitol, recognized as a promising renewable carbon source, is known to yield lactate in transition-metal-catalyzed dehydrogenation reactions.³⁵ Consequently, the reaction of sorbitol with benzyl alcohol provided **1b** with a decreased yield but a comparable TOF.

Conclusions

We introduce a sustainable catalytic process for the synthesis of diverse AHAs using biomass-derived C3 feedstocks such as glycerol, 1,2-propanediol, and sorbitol. In this process, Ir(triNHC) catalysts play a crucial role in producing AHAs with high TOFs. The feature of NHC ligands bound to the iridium ion significantly influences the rate of alcohol dehydrogenation, resulting in varied yields and TOFs. Beyond the impact of catalysts, the alcohol structure also contributes to differences in yields and TOFs; reactions involving benzyl alcohol derivatives exhibit faster rates than those with aliphatic alcohols, and the reactions of 1,2-propanediol proceed more rapidly than those of glycerol and sorbitol. The conversion of glycerol to AHAs involves four steps: (1) dehydrogenation of glycerol to form lactic acid, (2) dehydrogenation of lactic acid to produce pyruvic acid, (3) cross-coupling of pyruvic acid and aldehydes, and (4) reduction of cross-coupling intermediates. Based on the empirical results presented in Table 1 and control experiments, Ir(triNHC) catalysts play a crucial role in the dehydrogenation of alcohols and the C–C coupling reactions. The reduction of the cross-coupling intermediates is hypothesized to occur through base-mediated transfer hydrogenation and iridium-monohydride-mediated reduction.

Author contributions

H.-Y. Jang: conceptualization, supervision, writing original draft, and review & editing. H. Byeon, J. Kim, M.-h. Lee: investigation and formal analysis.

Conflicts of interest

There are no conflicts to declare.

Acknowledgements

This study was supported by the Carbon to X Program (No. 2020M3H7A1098283) and National Research Foundation Program (No. 2022R1A2C1004387) by the Ministry of Science and ICT, and the H2KOREA funded by the Ministry of Education (2022Hydrogen fuel cell-002), Innovative Human Resources Development Project for Hydrogen Fuel Cells.

References

- 1 M. Pagliaro, R. Ciriminna, H. Kimura, M. Rossi and C. D. Pina, *Angew. Chem., Int. Ed.*, 2007, **46**, 4434–4440.
- 2 C.-H. Zhou, J. N. Beltramini, Y.-X. Fan and G. Q. Lu, *Chem. Soc. Rev.*, 2008, **37**, 527–549.
- 3 A. Behr, J. Eilting, K. Irawadi, J. Leschinski and F. Lindner, *Green Chem.*, 2008, **10**, 13–30.
- 4 J. I. Garcia, H. Garcia-Marin and E. Pires, *Green Chem.*, 2014, **16**, 1007–1033.
- 5 M.-h. Lee, H. Byeon and H.-Y. Jang, *J. Org. Chem.*, 2022, **87**, 4631–4639.
- 6 J. Wu, L. Shen, Z.-N. Chen, Q. Zheng, X. Xu and T. Tu, *Angew. Chem., Int. Ed.*, 2020, **59**, 10421–10425.
- 7 Y.-Q. Zou, N. von Wolff, A. Anaby, Y. Xie and D. Milstein, *Nat. Catal.*, 2019, **2**, 415–422.
- 8 Q.-Q. Zhou, Y.-Q. Zou, Y. Ben-David and D. Milstein, *Chem. – Eur. J.*, 2020, **26**, 15487–15490.
- 9 Y.-Q. Zou, Q.-Q. Zhou, Y. Diskin-Posner, Y. Ben-David and D. Milstein, *Chem. Sci.*, 2020, **11**, 7188–7193.
- 10 S. Waiba, K. Maji, M. Miti and B. Maji, *Angew. Chem., Int. Ed.*, 2023, **62**, e202218329.
- 11 S. Tian, J. Li, X. Peng, Y. Xu, M. Wang, H. Tang, W. Zhou, M. Wang and D. Ma, *Sci. China: Chem.*, 2023, **66**, 2583–2589.
- 12 E. Gabirondo, A. Sangroniz, A. Etxeberria, S. Torres-Giner and H. Sardon, *Polym. Chem.*, 2020, **11**, 4861–4874.
- 13 H. Gröger, *Adv. Synth. Catal.*, 2001, **343**, 547–558.
- 14 J. J. Mills, K. R. Robinson, T. E. Zehnder and J. G. Pierce, *Angew. Chem., Int. Ed.*, 2018, **57**, 8682–8686.
- 15 V. R. Macherla, J. Liu, M. Sunga, D. J. White, J. Grodberg, S. Teisan, K. S. Lam and B. C. M. Potts, *J. Nat. Prod.*, 2007, **70**, 1454–1457.
- 16 K. Abrahamsson, P. Andersson, J. Bergman, U. Bredberg, J. Bränalt, A.-C. Egnell, U. Eriksson, D. Gustafsson,

K.-J. Hoffman, S. Nielsen, I. Nilsson, S. Pehrsson, M. O. Polla, T. Skjaeret, M. Strimfors, C. Wern, M. Ölwegård-Halvarsson and Y. Örtengren, *Med. Chem. Commun.*, 2016, **7**, 272–281.

17 G. E. Dobereiner and R. H. Crabtree, *Chem. Rev.*, 2010, **110**, 681–703.

18 Y. Obora, *ACS Catal.*, 2014, **4**, 3972–3981.

19 A. Corma, J. Navas and M. J. Sabater, *Chem. Rev.*, 2018, **118**, 1410–1459.

20 R. H. Crabtree, *ACS Sustainable Chem. Eng.*, 2019, **7**, 15845–15853.

21 M. Trincado, J. Böksen and H. Grützmacher, *Coord. Chem. Rev.*, 2021, **443**, 213967.

22 M. Huang, J. Liu, Y. Li, X.-B. Lan, P. Su, C. Zhao and Z. Ke, *Catal. Today*, 2021, **370**, 114–141.

23 J. G. Solsona, P. Romea, F. Urpi and J. Vilarrasa, *Org. Lett.*, 2003, **5**, 519–522.

24 H. Nagai, Y. Morita, Y. Shimizu and M. Kanai, *Org. Lett.*, 2016, **18**, 2276–2279.

25 G. Tang and C.-H. Cheng, *Adv. Synth. Catal.*, 2011, **353**, 1918–1922.

26 Y.-J. Cheong, K. Sung, J.-A. Kim, Y. K. Kim and H.-Y. Jang, *Eur. J. Inorg. Chem.*, 2020, 4064–4068.

27 K. Sung, M.-h. Lee, Y.-J. Cheong, Y. K. Kim, S. Yu and H.-Y. Jang, *Adv. Synth. Catal.*, 2021, **363**, 3090–3097.

28 M.-h. Lee, H. Byeon, S. Kim, W. Yoon, J. Park, H. Yun, S. Yu and H.-Y. Jang, *ACS Sustainable Chem. Eng.*, 2023, **11**, 8901–8907.

29 L. S. Sharninghausen, J. Campos, M. G. Manas and R. H. Crabtree, *Nat. Commun.*, 2014, **5**, 5084–5092.

30 Y.-J. Cheong, K. Sung, S. Park, J. Jung and H.-Y. Jang, *ACS Sustainable Chem. Eng.*, 2020, **8**, 6972–6978.

31 Y.-D. Long and Z. Fang, *Biofuels, Bioprod. Biorefin.*, 2012, **6**, 686–702.

32 M. Avramoff and V. Sprinzak, *J. Am. Chem. Soc.*, 1958, **80**, 493–496.

33 V. Polshettiwar and R. S. Varma, *Green Chem.*, 2009, **11**, 1313–1316.

34 J. A. Cabeza, M. Damonte, P. García-Álvarez and E. Pérez-Carreño, *Chem. Commun.*, 2013, **49**, 2813–2815.

35 M. G. Manas, J. Campos, L. S. Sharninghausen, E. Lin and R. H. Crabtree, *Green Chem.*, 2015, **17**, 594–600.

